Histol Histopathol (2009) 24: 693-706

http://www.hh.um.es

Histology and Histopathology

Cellular and Molecular Biology

Microvascular adaptive changes in experimental endogenous brain gliomas

Susana Bulnes[1], Juan Bilbao[2] and José Vicente Lafuente[1]

[1]Laboratory of Clinical and Experimental Neuroscience (LaNCE), Department of Neuroscience, Basque Country University, Leioa, Spain and [2]Department of Preventive Medicine and Public Health, School of Medicine and Dentistry, Basque Country University, Leioa, Spain

Summary. Glioma growth depends on microvascular adaptation and angiogenesis. Our study focused on the structural changes that occur in the microvasculature to adapt to glioma growth.

Vascular morphology, morphometry and permeability studies were performed in induced rat gliomas. Tumours were identified by magnetic resonance imaging and histopathology. Blood brain barrier integrity was examined by EBA and GluT-1 immunostaining and correlated with vascular permeability for gadolinium and intravital dyes. $VEGF_{165}$ immunoexpression was also analyzed.

Tumours were grouped in microtumours (6.69±0.99 mm^3) displaying a homogeneous T2-w hyperintense signal corresponding to low-grade gliomas, and macrotumours (900.79±332.39 mm^3) showing gadolinium contrast enhancement, intravital dye extravasation and histopathological features of high-grade gliomas.

Results show that the microvascular network becomes aberrant as we move from micro to macrotumours. Vessel density decreases, whereas the relative area occupied by the vascular network increases. Microtumours display homogeneous angioarchitecture composed of simple and mildly dilated vessels similar to normal tissue. Macrotumours show different patterns, following a gradient from the neoangiogenic border to the hypoxic core. The tumour core contains scarce, huge, dilated vessels with some profiles co-expressing GluT-1 and $VEGF_{165}$, the *peripheral* tissue shows light dilated vessels co-expressing EBA and GluT-1, and the *border area* displays glomeruloid vessels strongly positive for VEGF. Glucose uptake was maintained for some vascular endothelial sections in areas where BBB function was lost.

In conclusion, during development of gliomas the microvasculature becomes aberrant, undergoing a sequence of adaptive changes which involve the distribution and permeability of vessels. This explains the disturbances of blood flow and the increased permeability.

Key words: Angiogenesis, Blood brain barrier (BBB), Ethylnitrosourea (ENU), Gliomas, Microvascular network.

Offprint requests to: Dr. Jose Vicente Lafuente, Laboratory of Clinical and Experimental Neuroscience (LaNCE), Department of Neurosciences, Basque Country, Barrio Sarriena s/n, 48940 Leioa, Spain. e-mail: onbbuses@lg.ehu.es (SB), josevicente.lafuente@lg.ehu.es (JVL)

Introduction

The development of solid neoplasms has a close relationship with adequate oxygen delivery. The growth and survival of gliomas, the most common type of primary brain tumour, depends on vascular remodeling and angiogenesis (Folkman, 2000); these tumours form in highly-vascularized tissue. However, when the metabolic supply has been exceeded during neoplastic progression, vessel genesis becomes necessary (Carmeliet and Jain, 2000; Yancopoulos et al., 2000). Tissular hypoxia occurs when the vascular network cannot satisfy cell requirements, and this situation triggers the synthesis of vascular endothelial growth factor (VEGF) (Jin et al., 2000; Marti et al., 2000; Semenza, 2003). VEGF plays a pivotal role, inducing angiogenesis and increasing vascular permeability (Ferrara et al., 2003).

Endothelial cells of brain capillaries are the morphological substrate of the blood brain barrier that separates the brain from the exterior in order to maintain cerebral homeostasis. The lack of fenestrations and the presence of numerous tight junctions (TJs) in the interendothelial cleft differentiate brain microvessels from those of peripheral microvasculature. Tumour blood vessels have multiple abnormalities that result in a heterogeneous environment. They are disorganized, tortuous, sinusoidal, branchy and leaky, the diameter is irregular and the walls are thinner than those found in healthy brain tissue (Bigner et al., 1998). Endothelial cells of tumour vessels do not form a closed barrier, and pericytes are loosely attached (Baluk et al., 2005). Defective TJs explain the tumour vessel leakiness which leads to blood brain barrier (BBB) breakdown and the oedema associated with brain tumours (Hashizume et al., 2000; Papadopoulos et al., 2004).

The BBB is the set of physical and metabolic mechanisms regulating the passage of substances between the blood flow and the nervous parenchyma. Most of these mechanisms are involved in permeability regulation and are based on endothelial cells. This BBB permeability leads to extravasation of plasma proteins into brain parenchyma corresponding to an enhancement of the edematous fluid (Huber et al., 2001; Harhaj and Antonetti, 2004). In experimental models, vascular permeability has been detected by extravasation of intravital tracers such, as Evans Blue (Lafuente et al., 1994, Lafuente, 2004; Machein et al., 2004) or Rose Bengal (Yao et al., 2003). MRI enhanced with contrast media has also been used to study vascular permeability in tumours (Brasch and Turetschek, 2000; Roberts et al., 2000a,b). However, although gadolinium (Gd-DTPA) is a useful contrast medium to highlight increased permeability in malignant tumours, it is poorly suited for characterizing microvessels (Quarles and Schmainda, 2007).

On the other hand, some studies have been conducted to quantify the vasculature, using methods such as butyrylcholinesterase histochemistry (Argandona and Lafuente, 1996), alkaline phosphatase histochemistry (Fonta and Imbert, 2002), lectin histochemistry for LEA (Mazzetti et al., 2004; Argandona et al., 2005; Bengoetxea et al., 2008), immunohistochemistry against the glucose transporter-1 (GluT-1) (Dobrogowska and Vorbrodt, 1999) and Factor VIII antigens or the endothelial barrier antigen (EBA) (Lin and Ginsberg, 2000; Zhu et al., 2001; Krum et al., 2002).

Changes in vascular morphology, BBB permeability and angiogenesis during progression of cerebral tumours have been studied experimentally by brain injection of C6 cells (Holash et al., 1999; Vajkoczy et al., 2002) or by cerebral xenotransplants (Cha et al., 2003). All of these models develop tumours in healthy hosts, these being the providers of the vascular network. The present study has been conducted on an endogenous model of brain tumour that reproduces quite closely the whole oncological disease.

To date, little attention has been paid to the different stages of vasculature by those interested in glioma development. To address this question, we have been using a model of neurocarcinogenesis in which brain gliomas develop several months after a single prenatal exposure of rats to N-ethyl-N-nitrosourea (ENU). The aim of this work is to study the morphology of the microvascular network, from early to advanced stages of endogenously-induced rat gliomas, in order to elucidate changes related to the angiogenic switch. This information will help us to understand the effectiveness of parenteral treatments, when success or failure of therapies is linked to secondary changes in tumour growth.

Material and methods

Tumours were induced in Sprague Dawley rats by transplacentary exposure of litters to the carcinogen Ethylnitrosourea (ENU). 8 Dams were intraperitoneally injected with N-nitroso- N-ethylurea (10mg/ml in 0.9% NaCl, Ref.: E2129, Sigma-Aldrich, Spain), 80mg/kg of body weight, on the 15th day of pregnancy. Offspring rats exposed to ENU were reared in standard laboratory conditions. The study was performed on 55 rats from 6 months to one year of age.

All animal experiments were performed in accordance with the European Community Council Directive of 24 November 1986 (86/609/EEC).

Tumour screening

Intracerebral glial tumours were selected by magnetic resonance imaging (MRI, Biospec BMT 47/40, Bruker, Ettlingen, Germany, operating at 4.7 Tesla) taking into account the size, topographic location and intensity of the signal on T2-w and T1-w images and by histopathology study from H&E staining as previously described (Bulnes and Lafuente 2007). The MRI technique is a useful tool to detect "in vivo" cerebral tumours in order to reduce the number of animals devoted to the study.

Animals were anesthetized with isofluorane and intraperitoneally injected with 1.5ml/kg.b.w. of gadolinium (Gd-DTPA, Magnevist, Schering AG, Berlin, Germany). Coronal and sagittal images on T2-w fast spin-echo (TR/ effective TE= 3000/60 ms) and on T1-w spin-echo sequence (TR/TE = 700/15 ms) were obtained immediately after contrast administration. Glioma volumes were evaluated as previously described, Machein et al. (2004).

Following MRI, rats received an i.v. injection of 28.5mg/kg.b.w. of Evans Blue (EB) (Sigma Aldrich E2129) or Rose Bengal (RB) (Sigma Aldrich R3877) dye solutions for the vascular permeability study. After thirty minutes, animals were transcardially perfused with 4% fresh paraformaldehyde. Then brains were removed and immersed in the same solution at 4ºC overnight. Some coronal sections, including the tumour, were embedded in paraffin wax and cut at 4 µm. Some others were stored in 30% sucrose in 0.1M PBS until the tissues sank, cut in slices of 80 µm and stored in free-floating chambers.

Histochemistry and immunohistochemistry

The angioarchitecture was studied by butyrylcholinesterase histochemistry (Ref.: B-3253, Sigma-Aldrich) conducted on free-floating sections according to Argandona and Lafuente (1996) and LEA histochemistry (*Lycopersicon esculentum*, Ref.: L-0651, Sigma-Aldrich, 5 µg/ml) on paraffin sections, following the ABC method (Argandona and Lafuente, 2000).

Immunohistochemistry assay, using the conventional ABC method (Elite ABC Kit, Vector Laboratories, Burlingame, CA) was carried out on paraffin sections for: Vascular endothelial growth factor (polyclonal anti-$VEGF_{165}$, Ref.: sc-152, Santa Cruz Biotechnology Inc., Germany, 1:75), blood barrier specific antibody (monoclonal anti-EBA, Ref.: SMI 71, Sternberger Monoclonals Inc, Baltimore, MD, USA, 1:1000) and glucose transporter-1 (polyclonal anti-GluT-1, Ref.: AB 1340, Chemicon International, CA, USA, 1:1000). The reaction product was developed by 3.3-diamino-benzidine (DAB) (Ref.: 8001, Sigma-Aldrich, 0.25 mg/ml) and H_2O_2 solution (0.01%).

Some sections were used to co-localize EBA and GluT-1 antigens by double indirect immunofluorescence. The sections were incubated overnight with the aforesaid primary antibodies and with the folloing secondary antibodies: fluorescein isothiocyanate (FITC) conjugated anti-mouse IgG (Ref.: F-9137, Sigma-Aldrich, 1:100) ad ytetra,etjyl rhodamine isothiocyanate (TRITC) conjugated anti-rabbit IgG (Ref.: T-6778, Sigma-Aldrich, 1:100). Finally, the sections were incubated with solutions of Hoechst 33258 (Sigma-Aldrich, 5 µg/ml) in distilled water during 10 minutes. Images were acquired with an Olympus Fluovie FV500 confocal microscope using sequential acquisition to avoid overlapping of fluorescent emission spectra.

Negative controls, omitting the primary antisera, were also included in each staining run.

Computer-assisted morphometry

Measurements of the microvascular network were made in the core areas of 26 gliomas and in 5 areas of parietal cortex. Two slices of 4 µm were serially cut, one was used for haematoxylin-eosin staining in order to identify tumour areas, deleting necrotic or hemorrhagic parts, and the other was devoted to morphometry. In this second slice LEA histochemistry, as previously described, was performed but the cromogen signal was intensified by adding 1.3% NH_4NiSO_4 and 1.6% $CoCl_2$ to the developing solution.

Photomicrographs were digitalized using an Olympus camera (CAMEDIA 3030) at 100x magnification (pixel size of 0.476 µm) and pretreated with Adobe Photoshop 8.0.1, deleting artefacts in order to quantify the tumour vascular structures. Blood vessel measurements were carried out using the Image J Program (1.34n). The parameters taken into account were: vascular density (Vd.- number of vascular profiles per mm^2 of tissue), total vascular area (Va.- mm^2 of surface occupied by vessels per mm^2 of tissue) and mean vascular area (Vm.- mean size of vascular sections for each type of vessel, expressed in μm^2). Results from this assay allowed us to classify gliomas according to vessel shapes and sizes.

Data analysis

All the statistical analysis was performed using SPSS statistical software (version 14.0 SPSS, Inc., Chicago, Illinois). Prior to analysis, the data were examined for normal distribution using the Kolmogorov-Smirnov test and for homogeneity of variances using Levene's test. ANOVA analysis was performed to study the differences among the morphometric parameters from the three different groups of vessels. Post hoc test used the DMS and Bonferroni correction for equal variances or Tamhane's T2 correction for unequal variances. An unpaired t test was used to analyze differences among the averages of tumour volumes, vessel density, vascular network area and vessel area. Data are described as mean ± SD. A p value less than 0.05 was considered statistically significant.

Results

MR T2-weighted images allowed us to identify 65 intracerebral glial tumours, growing in association with the subcortical white matter, segregated into micro and macrotumour groups. Microtumours (n=34), with sizes from 0.53mm^3 to 20mm^3 (mean volume of 6.69±0.99 mm^3), displayed a hyperintense signal on T2-w images (Fig. 1a-c). Their margins appeared well delimited from the adjacent normal brain and there was no evidence of necrosis or sensitivity to spin-echo images to suggest hemorrhagic or calcified components. No appreciable mass effect or oedema was noted around the tumour. According to the microtumour size, two patterns of gadolinium (Gd-DTPA) contrast enhancement were found: small masses without gadolinium enhancement on T1-w images (Fig. 1a', b') and tumours around 20 mm^3 with a mild hyperintense signal (Fig. 1c'). By histopathology, microtumours displayed an isomorphous cellular pattern typical of low-grade gliomas. Most of them were constituted by cells with rounded, homogeneous nuclei and clear cytoplasm (honeycomb pattern). Neoplastic proliferations (12 in five different animals), undetected by MRI and discovered only by haematoxylin-eosin, were also included in this group. Although some of the microtumours revealed small haemorrhages (Fig. 2a), no histopathological features of malignancy were found, and the isomorphous histology pattern was maintained. They were mostly classic oligodendrogliomas.

Macrotumours (n=31) with dimensions from 20 to 7626.91 mm^3 (mean value of 900.79±332.39 mm^3) were localized in brain convexities involving the cortex and subcortical structures, with some occupying the whole hemisphere and expanding across the corpus callosum (Fig. 1f) towards the contralateral hemisphere, in the way of highly infiltrative and aggressive gliomas. The homogeneity of the microtumour T2-w signal was lost, showing intratumour areas with both hyperintense and hypointense signals (Fig. 1d-f). These neoplastic masses also displayed a heterogeneous T1-w image of gadolinium enhancement (Fig. 1d'-f'). Most malignant gliomas showed an annular rim of gadolinium enhancement signal lining the neoplastic mass (Fig. 1f'). The tissue pattern corresponds to anaplastic oligodendrogliomas. Histopathology features, such as cellular anaplasia with atypical mitosis, endothelial proliferations, hemorrhagic areas, cysts and necrosis were predominant. The largest tumours corresponded to highly-infiltrative malignant gliomas that displayed diagnostic features of glioblastoma multiforme (GBM), such as macro-haemorrhages (Fig. 2b), prominent microvascular proliferation, macrocysts (Fig. 2c) and necrosis with pseudopallisading (Fig. 2d).

Microvascular network

Butyrylcholinesterase

The enzymatic activity of butyrylcholinesterase (BChE) was homogeneously detected in the rat vascular endothelium and it was maintained in different conditions. In the tumour tissue we observed an abundant capillary network and perivascular cells strongly positive for this enzyme. The angioarchitecture of microtumours was similar to normal brain parenchyma (Fig. 3a). Tumours near to 20 mm^3 in size showed dilated vessels and some tortuousness (Fig. 3b). The capillary distribution was quite regular throughout the tumour and an avascular peritumoural rim was sometimes observed. In contrast, macrotumours displayed a chaotic vascular organization related to histopathological heterogeneity (Fig. 3c). The largest macrotumours displayed various microvascular patterns corresponding to areas of different histological characteristics (Fig. 3d): 1) Intratumour pattern, scarce vessels displaying huge dilated lumen and an unusual branched configuration; 2) Peripheral area with dilated vessels similar to those in brain parenchyma; 3) Border area separating tumour and peritumoural tissue, with

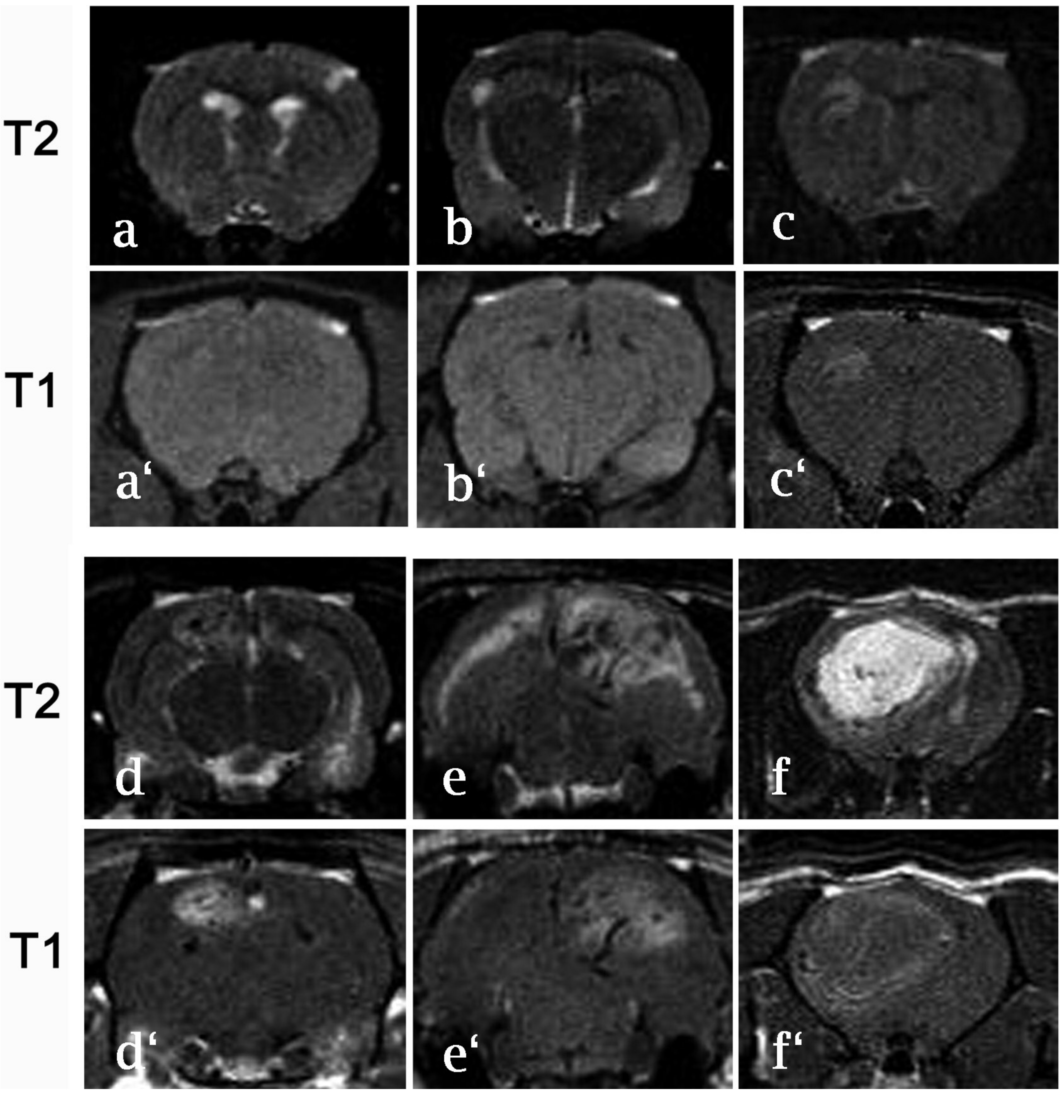

Fig. 1. Coronal sections of rat brains by MRI on T2-w and T1-w after injection of gadolinium. **a)** Small neoplastic mass with a homogeneous hyperintense signal on T2-w growing on the cortex; **(b)** tumour on subcortical white matter; **(a'-b')** both display an isointense signal on T1-w. **(c - c')** The pictures show a tumour of about 20 mm^3 displaying a hyperintense signal on both T2 and T1. **d - e**) Macrotumour with heterogeneous hyperintense signal on T2 and **(d´- e´)** after gadolinium injection. **f)** Highly-proliferative macrotumour covering a whole cerebral hemisphere. The T2-w images reveal an intratumoural hyperintense signal in the region occupied by a cyst. **f´)** The gadolinium enhancement shown on this T1-w image adopts a rim shape bordering the neoplastic mass.

numerous closely bunched small vessels. These results show a progression from homogeneous vascular distribution in microtumours to a disorganized and aberrant distribution in macrotumours. Remarkably, some strong positive cells were located around vessels constituting a cell sleeve.

Lycopersicon esculentum (LEA)

LEA glycoprotein was homogeneously present on all microvessels of normal and tumour tissue. LEA histochemistry depicted the complete microvascular network and also early changes in microglia. Its staining of the vascular network was very reproducible and consistent, with minimal background that enabled an easy identification of vascular profiles and quantification of the surface occupied by them. By classifying the microvascular profiles found in the gliomas by LEA histochemistry, the vessels were named and characterized as follows:

Tumour simple vessels (SV) (Fig. 4b), similar to the control tissue ones (Fig. 4a), displayed a mean size of 130±3.9 μm^2. *Dilated vessels* (DV) (Fig. 4c) of a mean size of 2125±695.2 μm^2 were characterized by incipient sinuosity. *Huge caliber vessels* (HCV) (Fig. 4d) with a size of 19615.13±3743.74 μm^2 showed a hyperplasic wall made up of several endothelial cell lines with a cube shape, and a thick basal membrane. Some sections of these huge vessels displayed patchy dye staining. *Endothelial proliferation* (EP) (Fig. 2a), showed a shape similar to Borist's rosettes from ependymoma. It consisted of several perivascular cell layers around the vascular lumen. *Glomeruloid vessels* (GV) (Fig. 4e), similar to human glioblastoma multiforme vessels, were characterized by numerous vascular lumina with a continuous endothelium sharing a basal membrane. Folding vascular structures (Fig. 4f) were similar to the glomeruloid vessels. They appeared in the intratumour

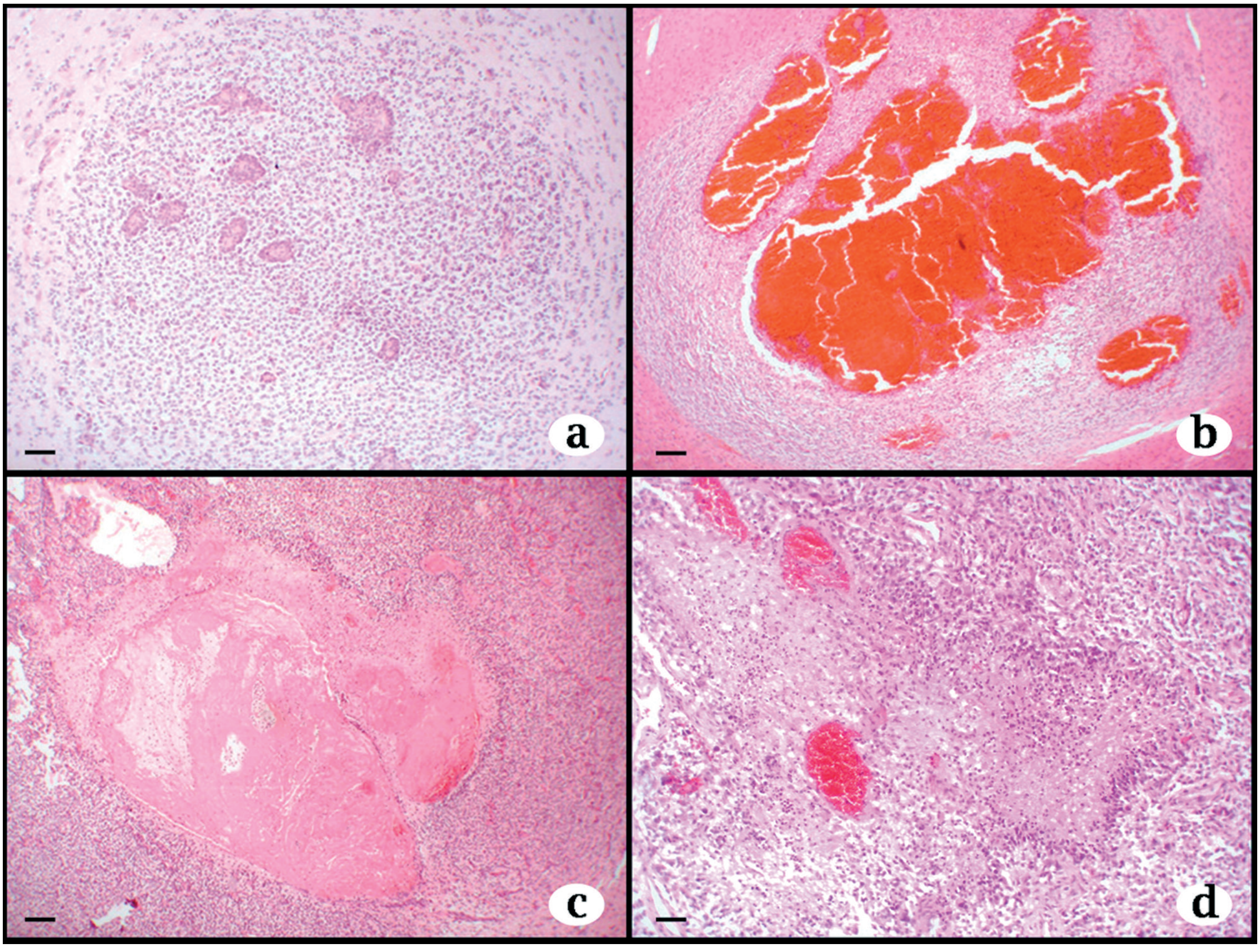

Fig. 2. Haematoxilin-eosin staining of gliomas showing histopathology features. **a.** Endothelial proliferations characteristic of gliomas near to 20 mm^3 in size. **b.** Macrohaemorrhages, macrocyst **(c)** and pseudopallisading necrosis **(d)** often found in macrotumour. Bar scale: 50 µm.

zones demarcating necrotic and perinecrotic areas.

Taking into account the location of the vessels described previously, it was found that simple and dilated vessels were a trait of microtumours, and vascular aberrant structures, such as huge, glomeruloid and folding vessels, were macrotumour features. Endothelial proliferations were observed in microtumours as well as in macrotumour cores. Simple vessels were homogenously distributed in small microtumours and cell proliferations and dilated vessels in microtumours around 20 mm^3. It is important to mention that these simple and dilated vessels were not exclusively found on microtumours, being frequently observed on the periphery of macrotumours. The microvascular network of the largest macrotumours showed variations related to the blood flow capacity of the different tumour areas. Between the core and the tumour border a gradient of changes in the vascular structures was found, from huge dilated vessels to normal ones in the peritumoural area.

Measurements of vessels were obtained from tumour areas already identified on HE slices. Briefly, SV are representative of neoplastic cell proliferations and small microtumours, DV of microtumours except for small ones, while HCV are representative of macrotumours. A comparative study of these three types of vessels and control vessels was made and the results are shown in Table 1. Vascular density and mean vascular area kept an inverse relationship throughout tumour development, and the surface occupied by tumour vessel sections increased according to glioma size. Vascular mean area decreased from *HCV* to control vessels but significant differences were only found for DV and *HCV* compared to controls ($p<0.05$). DV revealed a 37-fold higher

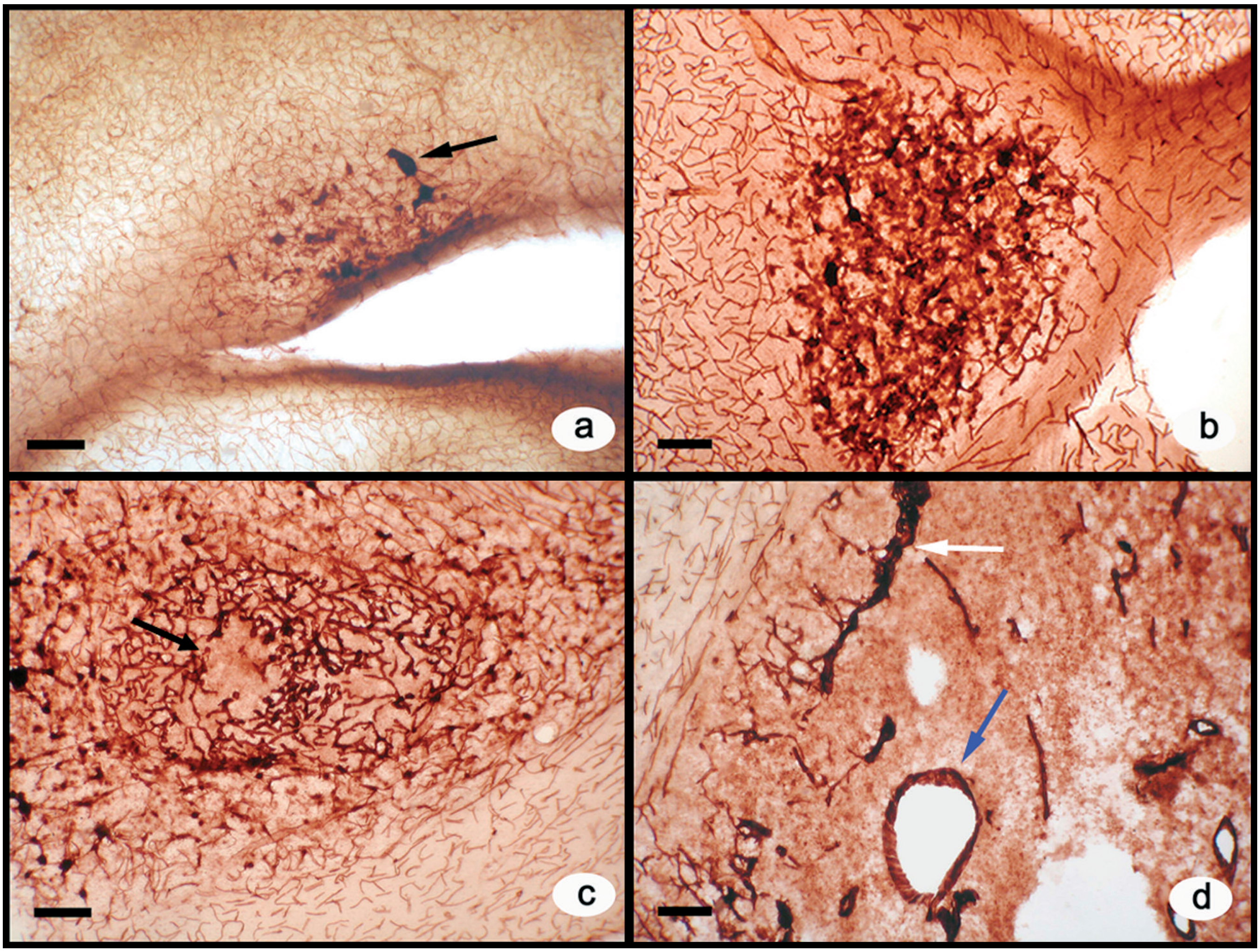

Fig. 3. Angioarchitecture of gliomas shown by butyrylcholinesterase histochemistry. **a.** Small mass showing some strongly-positive vessels for BChE (arrow). **b.** Tumour displaying a network of numerous capillaries of anarchic distribution. **c.** Macrotumour with avascular zone (black arrow) encircled by aberrant vessels. **d.** Malignant infiltrating macrotumour, with two aberrant vascular morphology patterns: intratumour pattern with scarce vessels of wide lumen (blue arrow) and peripheral area with numerous close vessels sharing a basal membrane (white arrow). Bar scale: 200 µm.

lumen area than controls and their network covered eleven percent of the neoplastic area. *HCV* were 150 times greater than SV and 350 times greater than controls. Neoplasm surface occupied by huge dilated vessels extended over 17% of the tumour area, similar to the dilated vessels and significantly higher than the area occupied by control or simple vessels.

BBB tracers

Evidence of gadolinium contrast enhancement *in vivo* or EB-RB dye extravasation *ex vivo* (Fig. 5A,B) appears in tumours around 20 mm^3. These exhibited mild homogeneous contrast enhancement on T1-w image (Fig. 5C). Macrotumours revealed irregular strong gadolinium enhancement as well as dye extravasation (Fig. 5D).

EBA, GluT-1 and VEGF

Vascular profiles from normal brain tissue were intensely and continuously labelled by EBA and GluT-1 as well as by LEA (Fig. 6i). The staining pattern of SV and DV for these markers was similar (Fig. 6j,k). Macrotumours revealed irregular and heterogeneous expression in vascular profiles for both BBB markers. Some tortuous vessels and DVs were unstained for EBA but they remained positive for GluT-1 (Fig. 6c,g,k). In

Table 1. The table shows the mean values (x ± SD).

Vessel type	Nº cases	Vd. (nº of vessels)	Va. (mm^2 network/tumour)	Vm. (μm^2)
Control	6	549±74.19	0.03±0.004	56.26±5.37
Simple vessel	15	293.53±39.854	0.035±0.008	130.22±32.97
Dilated	6	113.49±19.79	0.11±0.02	2,125.9±695.23
Huge caliber	5	23.73±8.13	0.17±0.03	19,615.13±3,743.74

Vascular density (Vd, number of vascular profiles per mm^2 of tumour); total vascular area (Va, mm^2 occupied by vessels per mm^2 of tumour); mean vascular area (Vm, mean size of vascular sections for each type of vessel, expressed in μm^2).

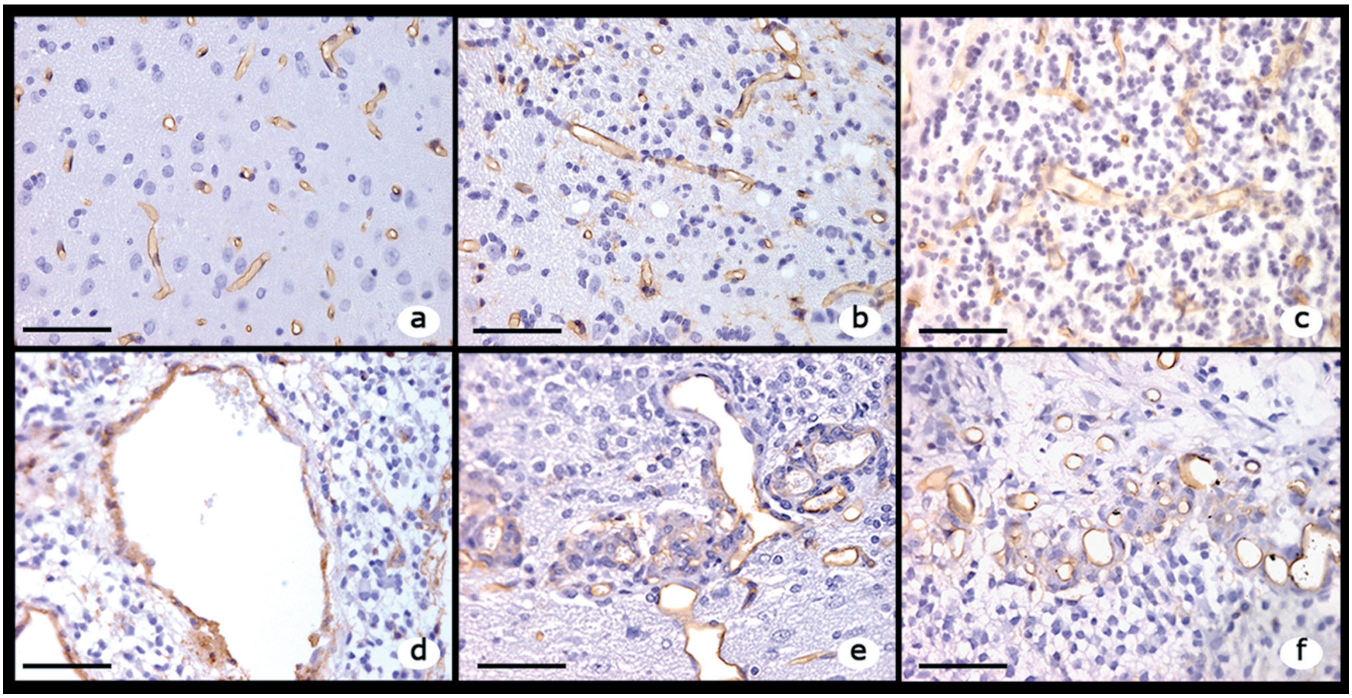

Fig. 4. Vascular profiles shown by LEA histochemistry. **a.** Microvessels of normal cerebral tissue. **b.** Microtumour blood vessel inside the neoplasia (called simple vessels), similar to the normal ones. **c.** Capillaries dilated inside tumour displaying a tortuous path. **d.** Huge dilated vessel with hyperplasic wall, their endothelial cells become cube-shaped. **e.** Glomeruloid vessels on the border of a macrotumour. **f.** Folding vascular structures like glomeruloid vessels limiting the peri-necrotic or peri-haemorrhagic area. These vascular structures separate areas of different interstitial tension. Bar scale: 50 µm.

HCV, in spite of not finding immunopositive vascular profiles for EBA, the GluT-1 immunostaining remained positive in a minority of vascular sections (Fig. 6d, h, l), occasionally co-expressing VEGF (Fig. 7a). Some endothelial proliferations (EP) in macrotumours showed VEGF-positive cells (Fig. 7b).

T1-w gadolinium enhancement in the most malignant and infiltrative gliomas displayed a rim with a hyperintense signal confined to the tumour border, like a ring. This area is mainly composed of glomeruloid vessels (Fig. 8A). Perinecrotic vessels were characterized by folding vascular structures. Both of these aberrant vascular structures, glomeruloid and perinecrotic vessels (Fig. 8B,C), had strong positivity for VEGF and usually co-expressed GluT-1 but not EBA (Fig. 8D). The microvascular endothelium from tumour borders was immunopositive for EBA antibody but surrounding haemorrhages or necrotic areas were unlabelled for this BBB antigen.

Discussion

This paper addresses some questions about microvascular morphology and remodeling features due

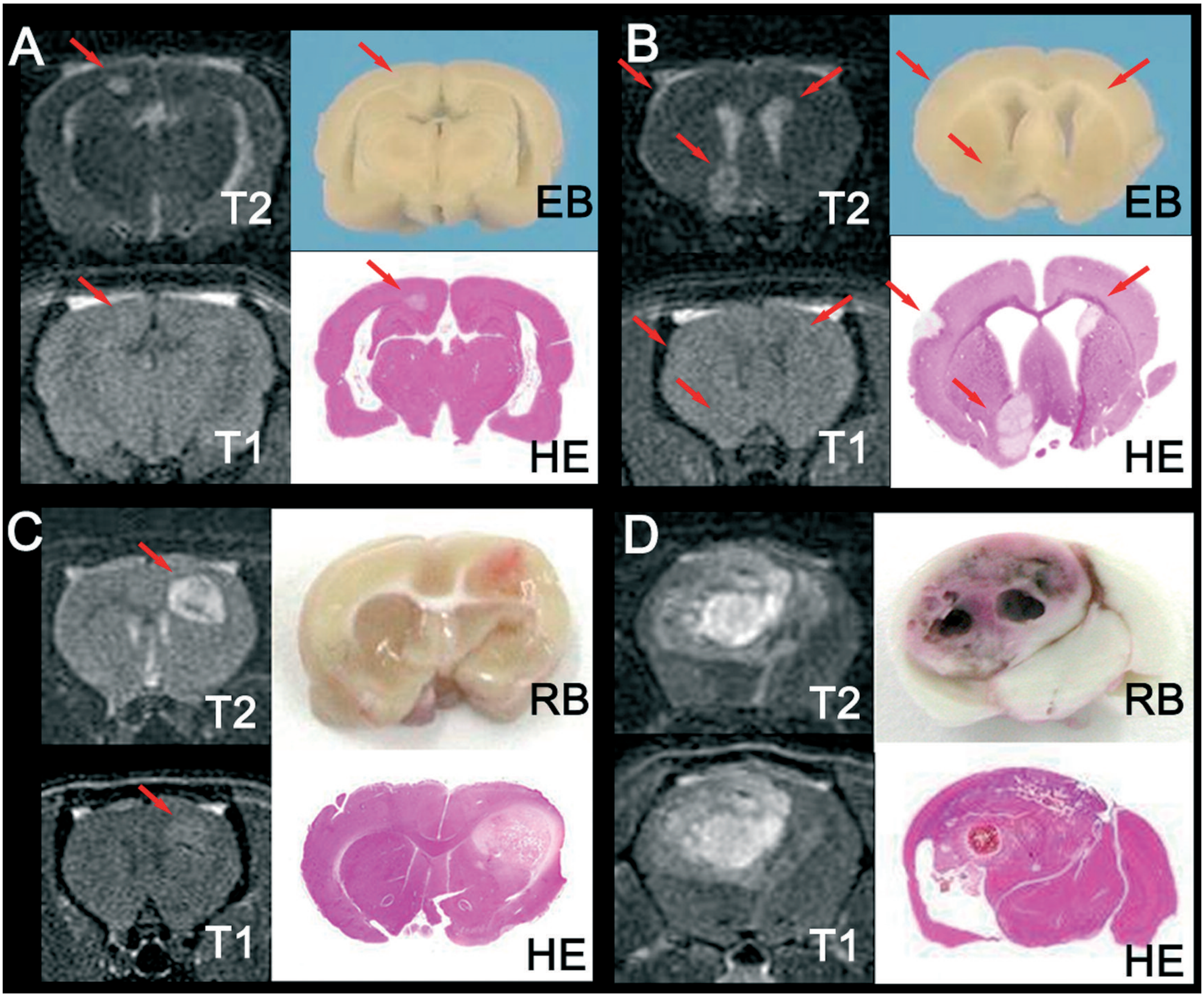

Fig. 5. Study of vascular permeability in micro and macrotumours taking into account intravital dye extravasation and gadolinium contrast enhancement signals. Coronal sections of rat brains are showed in vivo by MRI, at autopsy time by Evans Blue (EB) and Rose Bengal (RB) and histologically by haematoxylin eosin staining. **A, B.** Microtumours without contrast enhancement or Evans blue extravasation. **C.** Tumour displaying a mild hyperintense signal on T1 postcontrast and diffuse staining by Rose Bengal. **D.** Macrotumour showing heterogeneous dye staining and gadolinium signals on T1 image. This is due to haemorrhage and cysts shown in the histology section.

to glioma progression. Specifically, it defines some characteristics of vasculature in and around experimental endogenous gliomas.

Glioma transplacentary induction by ENU is a known and well establish model (Mennel et al., 2004; Slikker et al., 2004). It is well documented that ENU induces brain tumours mainly diagnosed as gliomas and schwannomas (Kish et al., 2001; Zook and Simmens, 2005; Bulnes-Sesma et al., 2006; Bulnes and Lafuente, 2007). For this study, we have selected only cerebral gliomas, based on the correlation between MR images and histopathology study. In previous works, we have shown that ENU induced microtumours over 6 months of extra-uterine life become nodular and around one year of age grow as a macrotumour toward the contralateral hemisphere. The microtumours studied were diagnosed as classic oligodendrogliomas, and the macrotumours as anaplastic oligodendrogliomas (Bulnes and Lafuente, 2007). The largest macrotumours, occupying a whole cerebral hemisphere or more, were very anaplastic, showing necroses with pseudopallisading, glomeruloid vessels, etc., all characteristics of glioblastoma multiforme (Kleihues et al., 2000; Brat and Van Meir, 2001). These results support the origin of GBM from an oligodendroglial cell lineage too. That could be relevant in human pathology, because oligodendrogliomas with deletion of 1p and 19q are sensitive to chemotherapy (Perry, 2001; Engelhard et al., 2002).

During glioma growth, the metabolic demand must be supplied by pre-existing vessels, and adaptation to new requirements leads to intrinsic vascular changes and to the generation of new vessels from pre-existing ones (Risau, 1997). When the proliferating cells outgrow the capacity of the regional vasculature to maintain

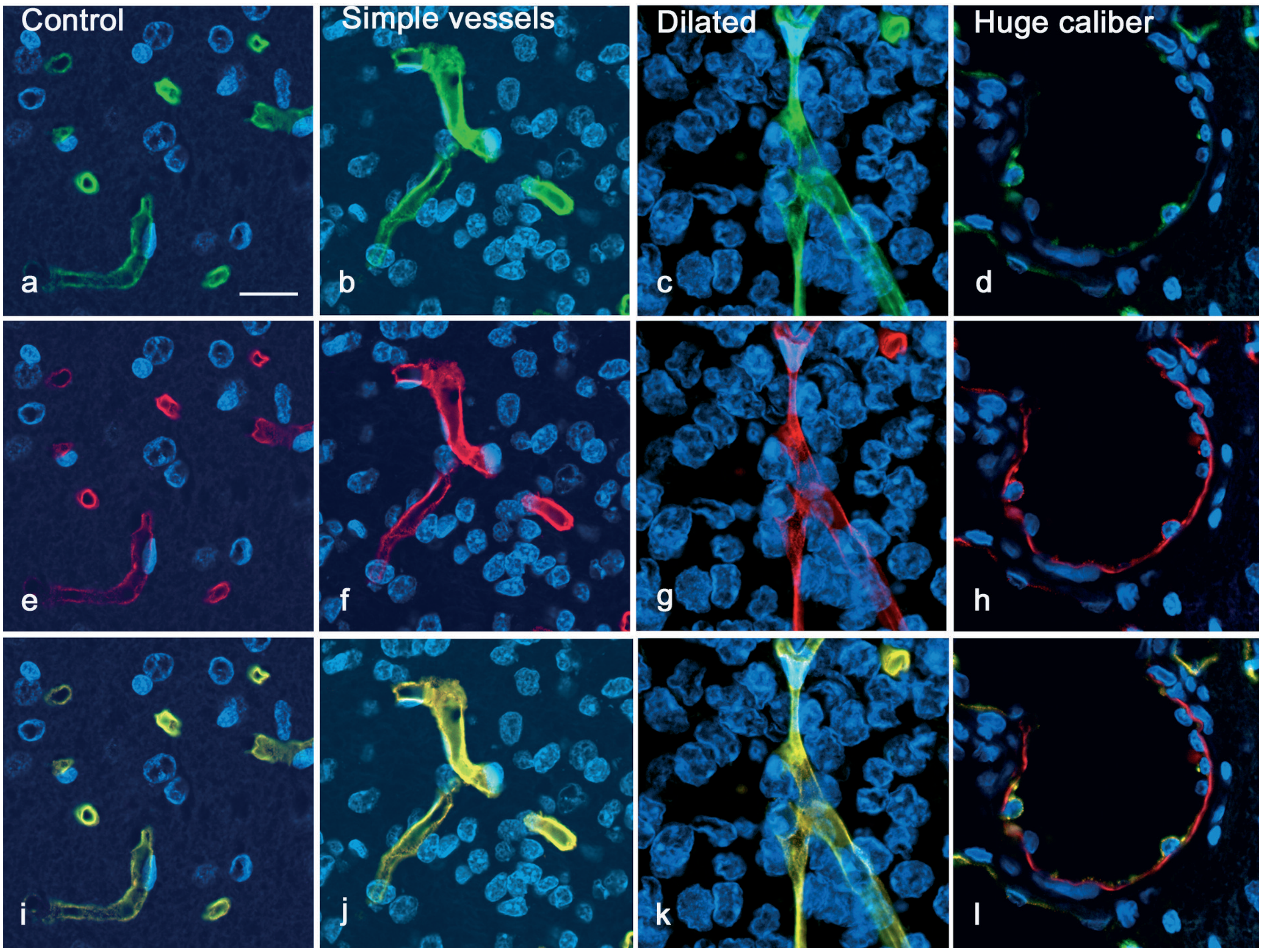

Fig. 6. Confocal microphotographs for EBA and GluT-1 double staining obtained by immunofluorescence with FITC (in green for the EBA, **a-d**) and TRITC (in red for the GluT-1, **e-h**); tumours were contrasted with Hoechst. **i-k**) Co-localized expression for both BBB markers in vascular profiles of simple and dilated tumour vessels (in yellow). **d.** Huge caliber vessels negative for EBA antibody with some vascular sections positive for GluT-1 (**h, l**). Scale bar: 20 µm.

homeostatic changes, the "angiogenic switch" is induced (Bergers and Benjamin, 2003). In the current study, vascular adaptations predominate over angiogenesis (Lafuente et al., 2000; Bian et al., 2006). This idea was supported by the adaptive changes of the microvasculature progression from low- to high-grade gliomas, which involved an increase in the tumour area occupied by the vascular network (Korkolopoulou et al., 2002). In accordance with the findings of Wesseling et al. (1998) on human gliomas, we have found a significant decrease in vascular density related to glioma malignancy, whereas tumour vascular area increases as a result of vessel dilatation. On the other hand, Korkolopoulou et al. (2002) reported an increase in vascular density in the same situation; but they selected the highest vascular field in GBM which, as in our model, corresponds with the neoangiogenic peripheral area. Therefore, this discrepancy could be due to this methodological difference.

Enzymatic activity for butyrylcholinesterase has been used to reveal changes in the angioarchitecture (Argandona and Lafuente, 1996), but in addition to this BChE activity is strongly related to neurogenesis and cellular proliferation (Mack and Robitzki, 2000), having a great role in tumourigenesis. Barbosa et al. (2001) reported the relationship between human glioma progression and BChE activity. They referred to a moderate activity of this esterase in grade II gliomas and high activity in grade III /IV gliomas. In our model, a progression from homogeneous to anarchic vascular

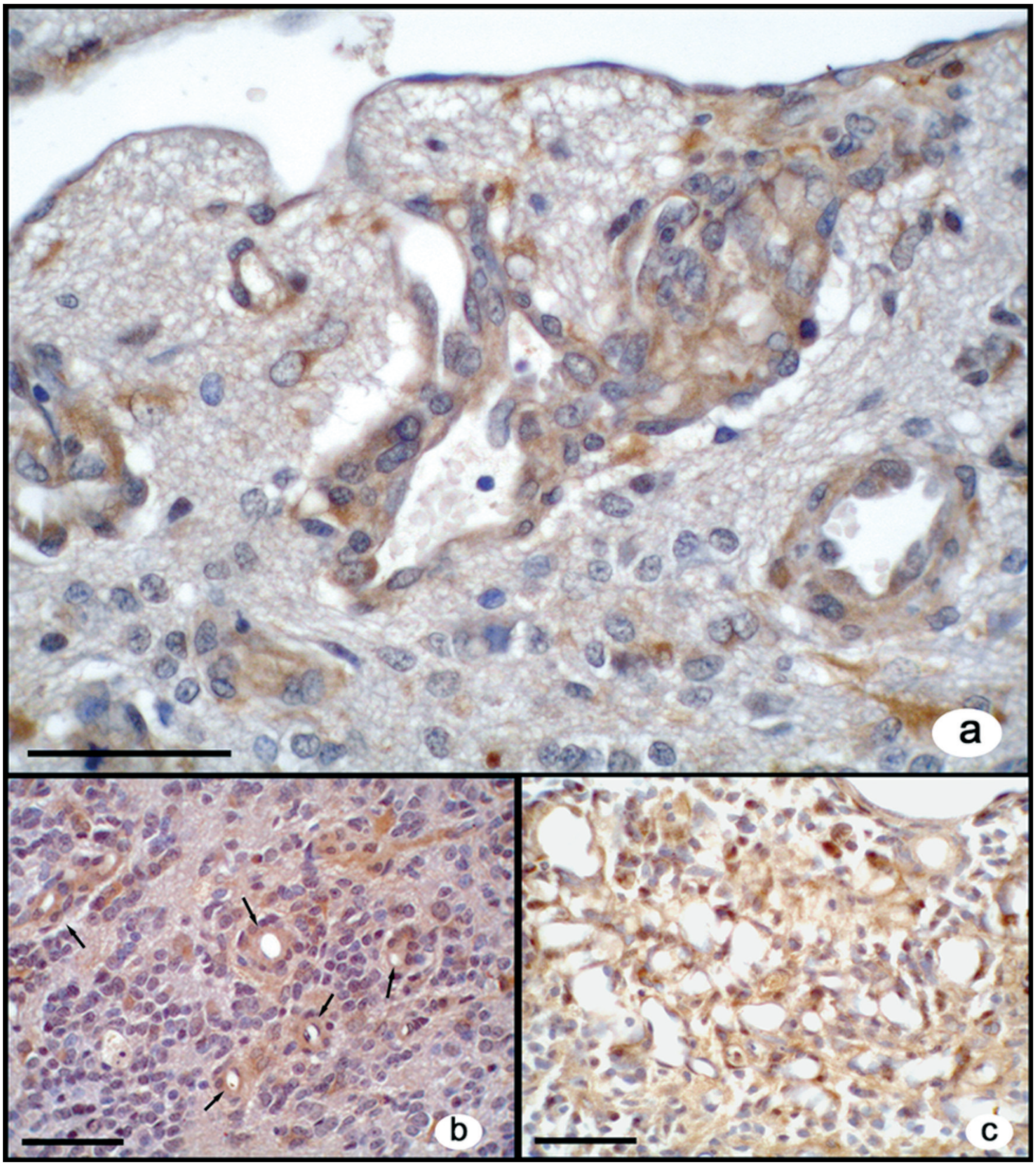

Fig. 7. $VEGF_{165}$ staining for the different aberrant vascular structures of the malignant macrotumours. **a.** Glomeruloid vessels on the tumour border, strongly-positive for this cytokine. **b.** Intratumour vascular proliferations positive for VEGF and **(c)** folding vascular structures like glomeruloid perinecrotic ones with some sections positive for VEGF Bar scale: 50 µm.

distribution, corresponding to low- and high-grade gliomas respectively, has been demonstrated. It is also worth mentioning that perivascular cells often displayed a high activity for BChE, depicted by a strong brown staining. These findings have led us to postulate that these perivascular cells might be stem cells proliferating around intratumour vessels (Brat et al., 2004; Anderson et al., 2005) and migrating through the vascular extracellular matrix (Ruoslahti, 2002).

Along the glioma progression there is a transition from the homogeneous capillary network to an anarchic angioarchitecture. There is a phase in tumour growth in which the microcirculation vessels acquire aberrant morphologies, becoming tortuous and dilated and displaying vascular leakage (Hashizume et al., 2000). Following this vascular aberration process, we have identified three vascular development stages: early, intermediate and advanced. The early vascular stage is constituted by simple vessels, the intermediate stage by tortuous and dilated vessels and the advanced stage by anarchic and aberrant vessels. These vascular development stages represent the ability of microvessels to adapt in order to maintain blood perfusion and metabolic support in adverse conditions, constituting a peculiar tissular microenvironment in response to hypoxia (Blouw et al., 2003).

The gradient from the well-oxygenated tumour periphery to the central hypoxic core is represented in

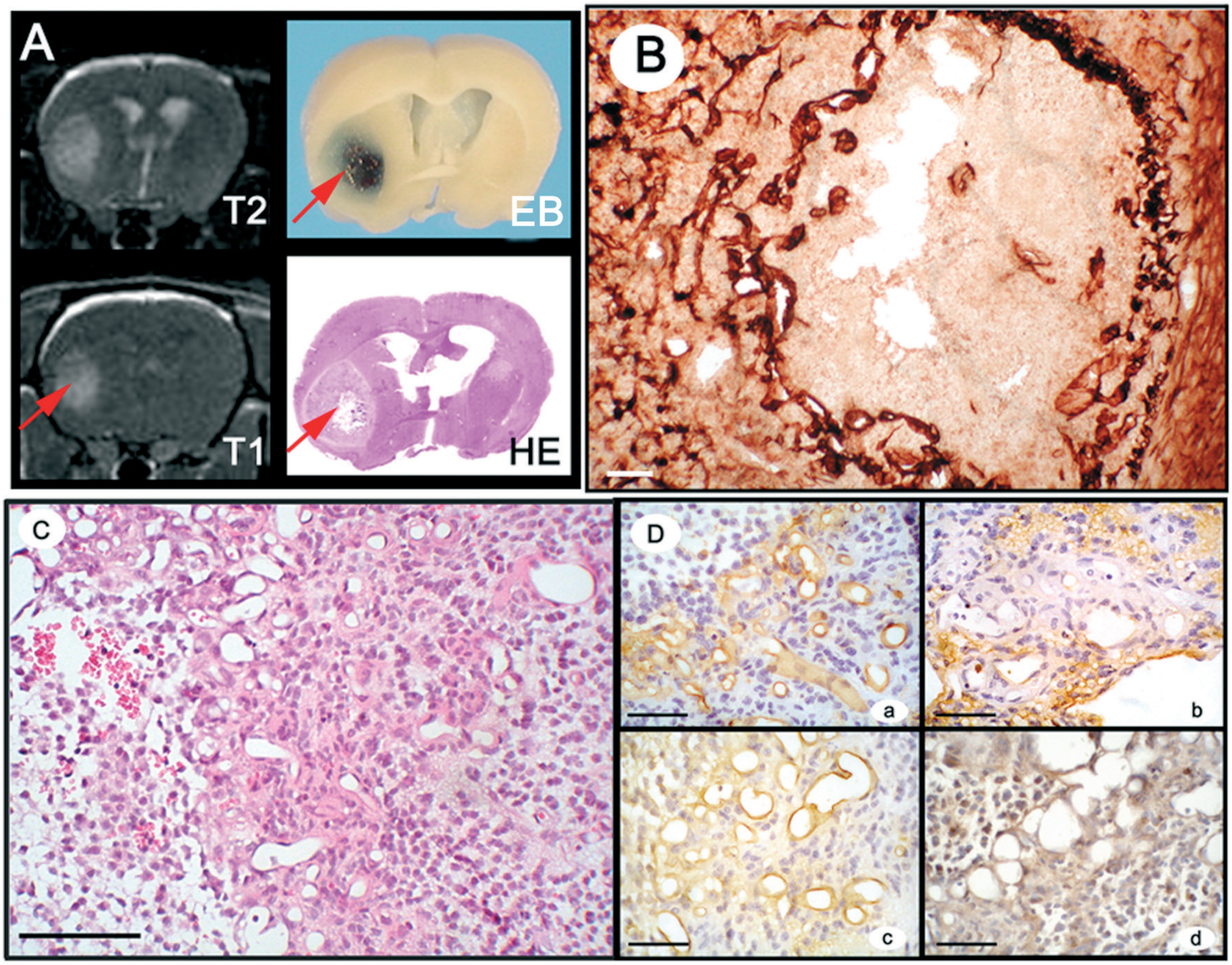

Fig. 8. Study of the vascular aberrant structures localized in the gadolinium (Gd-DTPA) enhancement signal area of macrotumours. **A.** Coronal sections of rat head by MRI on T2-w and T1-w postcontrast. The area of different intensity of gadolinium is shown by the red arrow. Corresponding brain section at autopsy time thirty minutes post Evans Blue (EB) dye i.p. injection and 4 µm slices of haematoxylin-eosin stain. **B.** Butyrylcholinesterase activity showed a strongly-positive vascular structure on the area studied. **C.** H&E corresponding with these vascular structures, showing numerous closely-bunched folded vessels. **D.** Histochemistry and immunohistochemistry study of vascular profiles. **a.** LEA stain. **b.** Lack of EBA immunopositivity. All vascular profiles express GluT-1 antigen **(c)** with co-expression of VEGF$_{165}$ **(d)**. Bar scale: B, 200 µm; C, D, 50 µm.

ENU high-grade gliomas. Dilated intratumoural vessels, expressing VEGF (Lafuente et al., 1999), increase their lumen on account of endothelial elongation but not of cell proliferation (Helmlinger et al., 2000). The intratumour area displays irregularly branching vessels, variable intravascular spaces and large avascular areas. Our results are in agreement with authors that consider the core of a high-grade glioma as an avascular zone, since it has scarce capillaries with wide lumen and a fragmented basal membrane, being rather inefficient for metabolic exchange (Vajkoczy and Menger, 2004). Cells adapted to hypoxic stress were clonally selected, and move toward the tumour periphery to infiltrate the parenchyma adjacent to the glioma (Fan et al., 2006; Jensen, 2006). In previous work we have shown that these cells co-express Ki-67 and VEGF (Bulnes and Lafuente, 2007).

ENU-induced glioblastomas develop two microvascular patterns closely related to tissue oxygenation. We found glomeruloid vessels positive for VEGF on the oxygenated peripheral area and huge dilated vessels with patchy staining for VEGF in the central hypoxic tumour zone. This cytokine not only triggers the angiogenesis process but also increases vascular permeability (Dvorak, 2006).

The increase of vascular permeability in this context could be due to the blood brain barrier dysfunction, to a structural break-down or to its immaturity. In pathological conditions, the BBB distortion and permeability increase has been related to intravital dyes extravasation, Gd-DTPA contrast enhancement on T1-w images (Cha et al., 2003; Claes et al., 2008) and to changes in the expression of BBB markers, such as EBA and GluT-1 (Sternberger et al., 1989; Zhu et al., 2001; Lafuente et al., 2006). This data support the view that only aberrant vessels in advanced stages lack the continuous EBA and GluT-1 expression.

Although dilated tortuous vessels of the intermediate vascular stage corresponding to non-anaplastic gliomas were stained for BBB markers and unstained for VEGF, these gliomas showed a homogeneous Gd-DTPA hyperintense signal and dye extravasation over the whole lesion. A possible explanation for the increased vascular permeability in these vessels could be the ultrastructural disruption of interendothelial tight junctions, without alterations of the BBB, mediated by growth factors such as VEGF (Ballabh et al., 2004). Furthermore, several researchers have stated that gadolinium enhancement and angiogenesis are two interconnected events (Brasch and Turetschek, 2000; Brasch et al., 2002). Perhaps in this early glioma development stage angiogenic switching can occur without alteration of the blood brain barrier function.

Malignant gliomas showed an uneven distribution of dyes and contrast and, as in human glioblastoma, a hyperintense rim on T1 surrounding the tumour. We were interested in elucidating the specific vascular structure of this rim and its BBB characteristics. Our findings showed two microvascular structures: aberrant folding microvascular structures and glomeruloid vessels. They lined two areas of different interstitial pressure: between the tumour and peritumoural areas and/or delimiting the necrotic or haemorrhagic area. We showed that glomeruloid vessels, in spite of being neoangiogenic and consequently immature vessels, express both BBB markers (EBA and GluT-1). Nevertheless, folding microvessels only keep the GluT-1 expression. These findings do not agree with Rosenstein et al. (1998), who associates VEGF expression with BBB dysfunction and the lack of GluT-1. According to Yeh et al. (2008) VEGF secreted by hypoxic neoplastic cells enhanced GluT-1 expression in brain endothelial cells, resulting in increased glucose uptake across the endothelium into surrounding cells. This enzymatic compensatory mechanism of the BBB represents a fundamental and critical adaptation needed for cellular homeostasis, and is necessary for brain tumour cells to survive and proliferate (Cornford and Hyman, 2005).

In conclusion, during development of these experimental gliomas the microvasculature undergoes a sequence of adaptive changes related to vascular distribution, as well as to the vessel wall, which explains blood flow distortion and increased permeability. These changes are similar to those manifested by human gliomas. Neoplasm causes an intratumour deficit of blood perfusion; it induces changes in vascular walls, including neoangiogenesis, remodeling and increase of vascular permeability by modification of the BBB in adapted vessels. Microvascular adaptations in early development stages are based on vasodilatation, endothelium elongation and permeability increase mediated by VEGF without BBB dysfunction. On the other hand, in malignant gliomas the microvascular adaptations vary according to blood flow perfusion. Permeability increase in intratumour vessels is not enough to supply the metabolic demand, and triggering of the angiogenesis process on the tumour border is necessary. This glioma model allows the sequential study of vascular aberrations. It may be useful in the design of vascular target therapies or antiangiogenic therapies to normalize the tumour vessels and recover normal blood flow.

Acknowledgements. This work has been partially supported by SAIOTEK (Department of Industry of the Basque Government), IT/460/07 (Basque Government), MSG G03/114, 9/212.327-1587 (University of the Basque Country EHU/UPV).

References

Anderson S.A., Glod J., Arbab A.S., Noel M., Ashari P., Fine H.A. and Frank J.A. (2005). Noninvasive MR imaging of magnetically labeled stem cells to directly identify neovasculature in a glioma model. Blood 105, 420-425.

Argandona E.G. and Lafuente J.V. (1996). Effects of dark-rearing on the vascularization of the developmental rat visual cortex. Brain. Res. 732, 43-51.

Argandona E.G. and Lafuente J.V. (2000). Influence of visual experience deprivation on the postnatal development of the microvascular bed in layer IV of the rat visual cortex. Brain Res. 855, 137-142.

Argandona E.G., Bengoetxea H. and Lafuente J.V. (2005). Lack of experience-mediated differences in the immunohistochemical expression of blood-brain barrier markers (EBA and GluT-1) during the postnatal development of the rat visual cortex. Brain Res. Dev. Brain Res. 156, 158-166.

Baluk P., Hashizume H. and McDonald D.M. (2005). Cellular abnormalities of blood vessels as targets in cancer. Curr. Opin. Genet. Dev. 15, 102-111.

Ballabh P., Braun A. and Nedergaard M. (2004). The blood-brain barrier: an overview: structure, regulation, and clinical implications. Neurobiol. Dis. 16, 1-13.

Barbosa M., Rios O., Velasquez M., Villalobos J. and Ehrmanns J. (2001). Acetylcholinesterase and butyrylcholinesterase histochemical activities and tumor cell growth in several brain tumors. Surg. Neurol. 55, 106-112.

Bengoetxea H., Argandona E.G. and Lafuente J.V. (2008). Effects of visual experience on vascular endothelial growth factor expression during the postnatal development of the rat visual cortex. Cereb. Cortex. 18, 1630-1639,

Bergers G. and Benjamin L.E. (2003). Tumorigenesis and the angiogenic switch. Nat. Rev. Cancer. 3, 401-410,

Bian X.W., Jiang X.F., Chen J.H., Bai J.S., Dai C., Wang Q.L., Lu J.Y., Zhao W., Xin R., Liu M.Y., Shi J.Q. and Wang J.M. (2006). Increased angiogenic capabilities of endothelial cells from microvessels of malignant human gliomas. Int. Immunopharmacol. 6, 90-99.

Bigner D.D., McLendon R.E., and Bruner J.M. (1998). Russell & Rubinstenin´s. Pathology of tumors of the nervous system. 6th ed. Arnold. London Blouw B., Song H., Tihan T., Bosze J., Ferrara N., Gerber H.P., Johnson R.S. and Bergers G. (2003). The hypoxic response of tumors is dependent on their microenvironment. Cancer. Cell 4, 133-146.

Brasch R. and Turetschek K. (2000). MRI characterization of tumors and grading angiogenesis using macromolecular contrast media: status report. Eur. J. Radiol. 34, 148-155.

Brasch R.C., Gossmann A., Helbich T.H., Kuriyama N., Roberts T.P., Shames D.M., van Bruggen N., Wendland M.F. and Israel M.A. (2002). Can a small-molecular gadolinium contrast agent be applied successfully with dynamic MRI to quantitatively define brain tumor microvascular responses to angiogenesis inhibition?. Acad. Radiol. 9 Suppl. 2, 326-327.

Brat D.J. and Van Meir E.G. (2001). Glomeruloid microvascular proliferation orchestrated by VPF/VEGF: a new world of angiogenesis research. Am. J. Pathol. 158, 789-796.

Brat D.J., Castellano-Sanchez A.A., Hunter S.B., Pecot M., Cohen C., Hammond E.H., Devi S.N., Kaur B. and Van Meir E.G. (2004). Pseudopalisades in glioblastoma are hypoxic, express extracellular matrix proteases, and are formed by an actively migrating cell population. Cancer Res. 64, 920-927.

Bulnes S. and Lafuente J.V. (2007). VEGF immunopositivity related to malignancy degree, proliferative activity and angiogenesis in ENU-induced gliomas. J. Mol. Neurosci. 33, 163-172.

Bulnes-Sesma S., Ullibarri-Ortiz de Z.N. and Lafuente-Sanchez J.V. (2006). Tumour induction by ethylnitrosourea in the central nervous system. Rev. Neurol. 43, 733-738.

Carmeliet P. and Jain R.K. (2000). Angiogenesis in cancer and other diseases. Nature 407, 249-257

Cha S., Johnson G., Wadghiri Y.Z., Jin O., Babb J., Zagzag D. and Turnbull D.H. (2003). Dynamic, contrast-enhanced perfusion MRI in mouse gliomas: correlation with histopathology. Magn. Reson. Med. 49, 848-855.

Claes A., Gambarota G., Hamans B., van T.O., Wesseling P., Maass C., Heerschap A. and Leenders W. (2008). Magnetic resonance imaging-based detection of glial brain tumors in mice after antiangiogenic treatment. Int. J. Cancer. Int. J. Cancer 122, 1981-1986.

Cornford E.M. and Hyman S. (2005). Localization of brain endothelial luminal and abluminal transporters with immunogold electron microscopy. NeuroRx. 2, 27-43.

Dobrogowska D.H. and Vorbrodt A.W. (1999). Quantitative immunocytochemical study of blood-brain barrier glucose transporter (GLUT-1) in four regions of mouse brain. J. Histochem. Cytochem. 47, 1021-1030.

Dvorak H.F. (2006). Discovery of vascular permeability factor (VPF). Exp. Cell Res. 312, 522-526.

Engelhard H.H., Stelea A. and Cochran E.J. (2002). Oligodendroglioma: pathology and molecular biology. Surg. Neurol. 58, 111-117.

Fan X., Salford L.G. and Widegren B. (2006). Glioma stem cells: Evidence and limitation. Semin. Cancer Biol. 17, 214-218.

Ferrara N., Gerber H.P. and LeCouter J. (2003). The biology of VEGF and its receptors. Nat. Med. 9, 669-676.

Folkman J. (2000). Tumour angiogenesis, in cancer medicine. In: Cancer medicine Hamilton. Hollan J.F., Frei E., Bast R.C., Kufe D.W., Pollock R.E. and Weichselbaum R.R. (eds). B.C. Decker Inc. Ontario, Canada. pp 132-152.

Fonta C. and Imbert M. (2002). Vascularization in the primate visual cortex during development. Cereb. Cortex. 12, 199-211.

Harhaj N.S. and Antonetti D.A. (2004). Regulation of tight junctions and loss of barrier function in pathophysiology. Int. J. Biochem. Cell Biol. 36, 1206-1237.

Hashizume H., Baluk P., Morikawa S., McLean J.W., Thurston G., Roberge S., Jain R.K. and McDonald D.M. (2000). Openings between defective endothelial cells explain tumor vessel leakiness. Am. J. Pathol. 156, 1363-1380.

Helmlinger G., Endo M., Ferrara N., Hlatky L. and Jain R.K. (2000). Formation of endothelial cell networks. Nature 405, 139-141.

Holash J., Maisonpierre P.C., Compton D., Boland P., Alexander C.R., Zagzag D., Yancopoulos G.D. and Wiegand S.J. (1999). Vessel cooption, regression, and growth in tumors mediated by angiopoietins and VEGF. Science 284, 1994-1998.

Huber J.D., Egleton R.D. and Davis T.P. (2001). Molecular physiology and pathophysiology of tight junctions in the blood-brain barrier. Trends Neurosci. 24, 719-725.

Jensen R.L. (2006). Hypoxia in the tumorigenesis of gliomas and as a potential target for therapeutic measures. Neurosurg. Focus. 20, E24.

Jin K.L., Mao X.O., Nagayama T., Goldsmith P.C. and Greenberg D.A. (2000). Induction of vascular endothelial growth factor and hypoxia-inducible factor-1alpha by global ischemia in rat brain. Neuroscience 99, 577-585.

Kish P.E., Blaivas M., Strawderman M., Muraszko K.M., Ross D.A., Ross B.D. and McMahon G. (2001). Magnetic resonance imaging of ethyl-nitrosourea-induced rat gliomas: a model for experimental therapeutics of low-grade gliomas. J. Neurooncol. 53, 243-257.

Kleihues P., Burger P.C., Collins V.P., Newcomb E.W., Ohgaki H. and Cavenee W.K. (2000). Glioblastoma. In: Pathology and genetics of tumours of the nervous system. Kleihues P. and Cavenee W.K. (eds). International Agency for Research on Cancer (IARC). Lyon.

pp 29-39.

Korkolopoulou P., Patsouris E., Kavantzas N., Konstantinidou A.E., Christodoulou P., Thomas-Tsagli E., Pananikolaou A., Eftychiadis C., Pavlopoulos P.M., Angelidakis D., Rologis D. and Davaris P. (2002). Prognostic implications of microvessel morphometry in diffuse astrocytic neoplasms. Neuropathol. Appl. Neurobiol. 28, 57-66.

Krum J.M., Mani N. and Rosenstein J.M. (2002). Angiogenic and astroglial responses to vascular endothelial growth factor administration in adult rat brain. Neuroscience 110, 589-604

Lafuente J.V. (2004). Involvement and consequences of Blood Brain Barrier permeability after minimal injury in rat cerebral cortex. In: Blood-spinal cord and brain barriers in health and disease. Sharma H.S. (eds). Elsevier Academic Press. San Diego, California. pp 533-545.

Lafuente J.V., Cervos-Navarro J. and Gutierrez Argandona E. (1994). Evaluation of BBB damage in an UV irradiation model by endogenous protein tracers. Acta Neurochir. Suppl. (Wien). 60, 139-141.

Lafuente J.V., Adán B., Alkiza K., Garibi J.M., Rossi M. and Cruz-Sánchez F.F. (1999). Expression of vascular endothelial growth factor (VEGF) and platelet-derived growth factor receptor-beta (PDGFR-beta) in human gliomas. J. Mol. Neurosci. 13, 177-185.

Lafuente J.V., Alkiza K., Garibi J.M., Alvarez A., Bilbao J., Figols J. and Cruz-Sanchez F.F. (2000). Biologic parameters that correlate with the prognosis of human gliomas. Neuropathology 20, 176-183.

Lafuente J.V., Argandona E.G. and Mitre B. (2006). VEGFR-2 expression in brain injury: its distribution related to brain-blood barrier markers. J. Neural. Transm. 113, 487-496.

Lin B. and Ginsberg M.D. (2000). Quantitative assessment of the normal cerebral microvasculature by endothelial barrier antigen (EBA) immunohistochemistry: application to focal cerebral ischemia. Brain Res. 865, 237-244.

Machein M.R., Knedla A., Knoth R., Wagner S., Neuschl E. and Plate K.H. (2004). Angiopoietin-1 promotes tumor angiogenesis in a rat glioma model. Am. J. Pathol. 165, 1557-1570.

Mack A. and Robitzki A. (2000). The key role of butyrylcholinesterase during neurogenesis and neural disorders: an antisense-5'butyrylcholinesterase-DNA study. Prog. Neurobiol. 60, 607-628.

Marti H.J., Bernaudin M., Bellail A., Schoch H., Euler M., Petit E. and Risau W. (2000). Hypoxia-induced vascular endothelial growth factor expression precedes neovascularization after cerebral ischemia. Am. J. Pathol. 156, 965-976.

Mazzetti S., Librizzi L., Frigerio S., de Curtis M. and Vitellaro-Zuccarello L. (2004). Molecular anatomy of the cerebral microvessels in the isolated guinea-pig brain. Brain Res. 999, 81-90.

Mennel H.D., Kosse N., Heverhagen J.T. and Alfke H. (2004). Primary and transplanted ENU induced rat tumors in neurooncology. Exp. Toxicol. Pathol. 56, 25-35.

Papadopoulos M.C., Saadoun S., Binder D.K., Manley G.T., Krishna S. and Verkman A.S. (2004). Molecular mechanisms of brain tumor edema. Neuroscience 129, 1011-1020.

Perry J.R. (2001). Oligodendrogliomas: clinical and genetic correlations. Curr. Opin. Neurol. 14, 705-710.

Quarles C.C. and Schmainda K.M. (2007). Assessment of the morphological and functional effects of the anti-angiogenic agent SU11657 on 9L gliosarcoma vasculature using dynamic susceptibility contrast MRI. Magn. Reson. Med. 57, 680-687.

Risau W. (1997). Mechanisms of angiogenesis. Nature 386, 671-674.

Roberts H.C., Roberts T.P., Brasch R.C. and Dillon W.P. (2000a). Quantitative measurement of microvascular permeability in human brain tumors achieved using dynamic contrast-enhanced MR imaging: correlation with histologic grade. Am. J. Neuroradiol. 21, 891-899.

Roberts T.P., Chuang N. and Roberts H.C. (2000b). Neuroimaging: do we really need new contrast agents for MRI? Eur. J. Radiol. 34, 166-178.

Rosenstein J.M., Mani N., Silverman W.F. and Krum J.M. (1998). Patterns of brain angiogenesis after vascular endothelial growth factor administration in vitro and in vivo. Proc. Natl. Acad. Sci. USA 95, 7086-7091.

Ruoslahti E. (2002). Specialization of tumour vasculature. Nat. Rev. Cancer 2, 83-90.

Semenza G.L. (2003). Targeting HIF-1 for cancer therapy. Nat. Rev. Cancer 3, 721-732.

Slikker W.3., Mei N. and Chen T. (2004). N-ethyl-N-nitrosourea (ENU) increased brain mutations in prenatal and neonatal mice but not in the adults. Toxicol. Sci. 81, 112-120.

Sternberger N.H., Sternberger L.A., Kies M.W. and Shear C.R. (1989). Cell surface endothelial proteins altered in experimental allergic encephalomyelitis. J. Neuroimmunol. 21, 241-248.

Vajkoczy P. and Menger M.D. (2004). Vascular microenvironment in gliomas. Cancer Treat. Res. 117, 249-262.

Vajkoczy P., Farhadi M., Gaumann A., Heidenreich R., Erber R., Wunder A., Tonn J.C., Menger M.D. and Breier G. (2002). Microtumor growth initiates angiogenic sprouting with simultaneous expression of VEGF, VEGF receptor-2, and angiopoietin-2. J. Clin. Invest. 109, 777-785.

Wesseling P., van der Laak J.A., Link M., Teepen H.L. and Ruiter D.J. (1998). Quantitative analysis of microvascular changes in diffuse astrocytic neoplasms with increasing grade of malignancy. Hum. Pathol. 29, 352-358.

Yancopoulos G.D., Davis S., Gale N.W., Rudge J.S., Wiegand S.J. and Holash J. (2000). Vascular-specific growth factors and blood vessel formation. Nature 407, 242-248.

Yao H., Sugimori H., Fukuda K., Takada J., Ooboshi H., Kitazono T., Ibayashi S. and Iida M. (2003). Photothrombotic middle cerebral artery occlusion and reperfusion laser system in spontaneously hypertensive rats. Stroke 34, 2716-2721.

Yeh W.L., Lin C.J. and Fu W.M. (2008). Enhancement of glucose transporter expression of brain endothelial cells by vascular endothelial growth factor derived from glioma exposed to hypoxia. Mol. Pharmacol. 73, 170-177.

Zhu C., Ghabriel M.N., Blumbergs P.C., Reilly P.L., Manavis J., Youssef J., Hatami S. and Finnie J.W. (2001). Clostridium perfringens prototoxin-induced alteration of endothelial barrier antigen (EBA) immunoreactivity at the blood-brain barrier (BBB). Exp. Neurol. 169, 72-82.

Zook B.C. and Simmens S.J. (2005). Neurogenic tumors in rats induced by ethylnitrosourea. Exp. Toxicol. Pathol. 57, 7-14.

Accepted December 29, 2008